Thermodriven Conformational Transition of Optically Active Poly[2,7-{9,9-bis[(*S*)-2-methyloctyl]}fluorene] in Solution

Hong-Zhi Tang,[†,⊥] Michiya Fujiki,*[,†,‡,#] and Takahiro Sato[†,§]

CREST-JST (Japan Science and Technology Corporation), 4-1-8 Hon-cho, Kawaguchi, Saitama 332-0012, Japan; NTT Basic Research Laboratories, NTT Corporation, 3-1 Wakamiya, Morinosato, Atsugi, Kanagawa 243-0198, Japan; and Department of Macromolecular Science, Osaka University, 1-1 Machikaneyama, Toyonaka, Osaka 560-0043, Japan

Received March 4, 2002; Revised Manuscript Received May 21, 2002

ABSTRACT: We report the first solution state circular dichroism (CD) spectroscopic properties of a newly designed polyfluorene (PF) featuring highly enantiopure β-branched chiral alkyl side chains, poly[2,7-{9,9-bis[(*S*)-2-methyloctyl]}fluorene] (PFMO), in dilute THF solution. Upon cooling the solution temperature, the single positive-sign CD band at 380 nm at +50 °C gradually changed into an apparent bisignate CD signal with two extrema of 403 and 355 nm at −80 °C, while the broad UV−vis band centered at 380 nm changed into a major intense band at 399 nm with a shoulder around 380 nm. On the basis of these data combined with photoluminescence (PL) studies and viscometric measurement, we concluded that PFMO in THF solution underwent a certain thermodriven, order−disorder conformational transition around 0 °C. It was considered that, upon cooling, the randomly twisted local PF backbone motifs in the wormlike PF backbone at higher temperature were transformed into a highly ordered PF backbone motif, possibly a *P*-5_2 helix (the *P*-handedness is assumed here corresponding to the negative-sign CD band, and vice versa), and other unclear local backbone motifs with the opposite screw sense at lower temperature.

Introduction

π-Conjugated polymers are promising functional materials having potential applications such as light-emitting diodes,[1] plastic lasers,[2] photovoltaic cells,[3] thin film transistors,[4] and chemical sensors.[5] Among them, especially, polyfluorene (PF) has recently attracted increasing interest due to its bluish photo- and/or electroluminescence with high quantum yield, high hole mobility, and excellent thermal, chemical, and photochemical stabilities.[6−12]

Although much research attention has been paid to the elucidation of the PF backbone structure, the most probable conformational structure of the PF backbone is somewhat controversial. On the basis of the fiber diffraction X-ray scattering experiments, Grell et al. concluded that PF bearing *n*-octyl side chains, poly[2,7-(9,9-di-*n*-octyl)fluorene] (PFO), can assume a fully extended anti-coplanar structure.[7] However, Lieser et al. demonstrated that PF having racemic 2-ethylhexyl side chains, poly{2,7-[9,9-bis(2-ethylhexyl)]fluorene} (PFEH), favorably adopts a 5_2 helical structure rather than the other possible 5_1 helix by means of transmission electron microscopy (TEM), electron and X-ray diffractions, and molecular orbital calculations.[8] Moreover, from semiempirical Hartree−Fock (HF) calculations, Hong et al. suggested that the 9,9-unsubstituted PF, poly(2,7-fluorene) (HPF), is able to adopt both 5_1 and 5_2 helices.[9]

On the other hand, there have been several reports supporting a wormlike global structure of PF in solutions around room temperature. For example, based on UV−vis absorption spectra in THF at room temperature, poly[2,7-(9,9-di-*n*-hexyl)fluorene] (PFH) was indicated to have an effective conjugation length of about 12 fluorene repeat units,[10] corresponding to a persistence length, q, of ∼10 nm.[11] Similarly, PFO was characterized to have a q of ca. 8.5 nm from the light scattering experiment in THF at +40 °C.[7b] Recently, PFEH was reported to adopt a wormlike structure with a q of ca. 7 nm and a cross-section diameter, d, of ca. 1.8 nm, based on small-angle neutron scattering and translational diffusion measurements in toluene at +20 °C.[11]

Oda, Neher, and co-workers synthesized the first optically active PF bearing highly enantiopure chiral alkyl side chains, poly[2,7-{9,9-bis[(*S*)-3,7-dimethyloctyl]}-fluorene] (PFDMO).[12] They suggested that PFDMO may adopt helical backbone structures in an annealed thin film based on spectroscopic data including circular dichroism (CD), UV−vis, electroluminescence (EL), and circularly polarized electroluminescence (CPEL). However, any further information on the PF backbone conformation in solution has not been reported yet, due probably to the weakness of the CD signal in solution at room temperature.

To more clearly investigate PF conformational structure in the solution state, an optically active PF exhibiting an intense CD signal in solution even at room temperature is required. For this purpose, we have designed and synthesized a new PF, poly[2,7-{9,9-bis[(*S*)-2-methyloctyl]}fluorene] (PFMO, Scheme 1),[6d,e,10] on the assumption that the stereocenter at the β-position in the side chains would effectively induce a more chirally ordered PF backbone structure than that at the γ-position and that a longer side chain may afford greater solubility of PF in organic solvents even at lower temperatures.

† CREST-JST.
‡ NTT Basic Research Laboratories.
§ Osaka University.
⊥ Present address: Department of Materials Science and Engineering, Box 352120, University of Washington, Seattle, WA 98195-2120.
Present address: Graduate School of Materials Science, Nara Institute of Science and Technology (NAIST), 8916-5 Takayama, Ikoma, Nara 630-0101, Japan.
* To whom correspondence should be addressed. E-mail: fujikim@ms.aist-nara.ac.jp.

10.1021/ma020327f CCC: $22.00
Published on Web 06/26/2002

Scheme 1

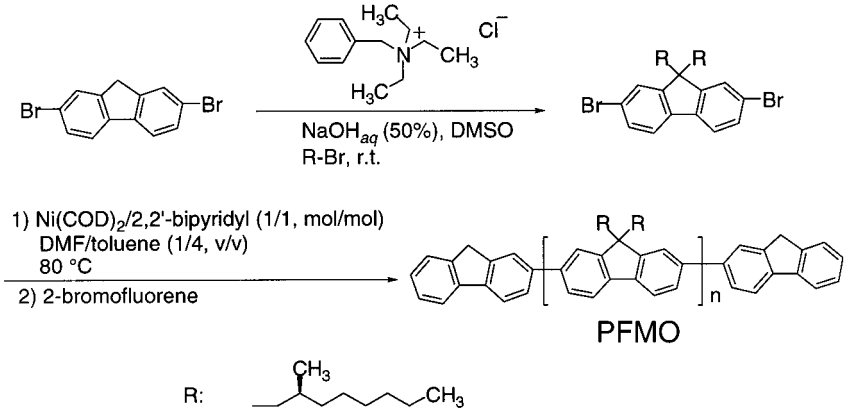

The present paper reports the first CD spectroscopic properties along with UV−vis, photoluminescence (PL), and photoluminescence excitation (PLE) spectra, and photoluminescence anisotropy (PLA) of PFMO in a molecularly dispersed solution state. On the basis of variable temperature CD and UV−vis measurements, photoluminescence studies, and viscometric measurements, we concluded that PFMO undergoes a certain thermodriven, order−disorder transition of conformational motifs with a weak cooperativity around 0 °C. This transition was discerned to be a significant thermodriven chiroptical change associated with thermochromism. The randomly twisted disordered motifs in the wormlike PF backbone at higher temperatures were considered to be transformed into a highly ordered PF motif, possibly a *P*-5_2 helix, along with additional plural motifs at lower temperatures.

Experimental Section

Materials. All commercial chemicals were used without further purification. Spectrophotometric grade THF (Kanto) was used for preparing polymer solutions for measurements. (*S*)-2-Methyloctyl bromide was synthesized at the Chemical Soft Co. (Kyoto, Japan) by bromination of (*S*)-2-methyl-1-octanol (Japan Energy, Tokyo, Japan, $[\alpha]^{25}_{D} = -9.6°$ (neat), ≥89% *e.e.* noted *in Chiral Reagents* 1600, p 213).

General. ^{1}H (300.0 MHz) and ^{13}C (75.4 MHz) NMR spectra were recorded in $CDCl_3$ at room temperature with a Varian Unity 300 NMR spectrometer using tetramethylsilane as an internal standard. Elemental analyses were performed at the Toray Research Center (TRC, Shiga, Japan) using a Vario elemental analysis apparatus. Optical rotation at the Na D line was measured with a JASCO DIP-370 polarimeter using a quartz cell with a path length of 1.0 cm at room temperature (23−24 °C). Molecular weights were evaluated by size exclusion chromatography (SEC) on a Shodex KF806M column (eluent THF, +30 °C) using a Shimadzu liquid chromatography instrument equipped with a photodiode array detector based on the calibration with polystyrene standards. CD and UV−vis absorption spectra were recorded simultaneously on a JASCO J-725 spectropolarimeter equipped with a Peltier control for temperatures from +80 to −10 °C (cell path: 1.0 or 0.1 cm) and a liquid nitrogen-controlled quartz cell with a path length of 0.5 cm in a cryostat, ranging from −20 to −80 °C. PL and PLE spectra were collected from the front surface of a quartz cuvette (0.5 cm) or a thin film on a quartz substrate in 45°/45° angle geometry to minimize the self-absorption effects due to high optical densities using a Hitachi 850 spectrofluorometer equipped with a Daikin cryotec control for temperatures from 24 to −80 °C. PLA was measured using a quartz cell with a path length of 1.0 cm in right angle geometry.

Syntheses. The synthetic procedure is outlined in Scheme 1. Using the phase transfer catalyst, triethylbenzylammonium chloride (Kanto), the monomer, 2,7-dibromo-9,9-bis[(*S*)-2-methyloctyl]fluorene, was synthesized from 2,7-dibromofluorene (Aldrich) and (*S*)-2-methyloctyl bromide in a high yield of 90%.[6d,e] Polymerization was carried out using a zerovalent nickel reagent, bis(1,5-cyclooctadiene)nickel(0) ($Ni(COD)_2$) (Kanto), and the end termination was accomplished using 2-bromofluorene (Acros).[6d,e,10]

2,7-Dibromo-9,9-bis[(*S*)-2-methyloctyl]fluorene: $[\alpha]^{24}_{D} = -1.5°$ (neat). ^{13}C NMR: δ (ppm) 14.10, 21.67, 22.66, 26.25, 28.84, 29.22, 31.73, 38.28, 47.98, 55.29, 121.06, 121.14, 127.20, 130.14, 139.16, 152.56. Calcd for $C_{31}H_{44}Br_2$: C, 64.59; H, 7.69. Found: C, 64.65; H, 7.60%.

PFMO: ^{13}C NMR: δ (ppm) 14.09, 22.02, 22.68, 26.63, 29.11, 29.40, 31.78, 38.87, 48.42, 55.06, 119.90, 122.68, 126.21, 140.21, 140.36, 151.55. Calcd for $C_{31}H_{44}$: C, 89.36; H, 10.64. Found: C, 88.74; H, 10.70%. $M_w = 56\,600$, $M_n = 18\,300$. PFMO was readily soluble in organic solvents such as THF, chloroform, and toluene.

Viscosity. Intrinsic viscosity−molecular weight relationships in THF and in toluene were performed using an in-line configuration of a viscometer (Viscotek T60A) and the SEC (Shimadzu) instrument described previously and an in-line configuration of a viscometer (Viscotek H502a, equipped with a capillary of the dimensions 0.5 mm i.d. × 61 cm length) and SEC (Waters 150C) at TRC, respectively. The Mark−Houwink−Sakurada equation obtained for PFMO were $[\eta] = 0.70 \times 10^{-5} M^{1.07}$ in THF at +30 °C and $[\eta] = 8.92 \times 10^{-5} M^{0.82}$ in toluene at +30 °C.

Spectrum Deconvolution. The peak fitting of the UV−vis spectrum was performed using scientific graphing and analysis software, Origin, version 6.1 (OriginLab Corporation, Northampton, MA), with a Gaussian peak function.

Results and Discussion

Chiroptical Properties. Figure 1 shows the variable temperature CD and UV−vis spectra of PFMO in THF.[13] The CD spectrum at +50 °C exhibits a positive-sign CD signal ($\Delta\epsilon = 2.1$ (FL-repeat-unit)$^{-1}$ dm^3 cm^{-1}), matching the maximum of the corresponding UV−vis absorption ($\lambda_{max} = 380$ nm, $\epsilon = 3.35 \times 10^4$ (FL-repeat-unit)$^{-1}$ dm^3 cm^{-1}) due to the π−π^* transitions of the PF backbones, indicating that PFMO may assume a certain chiral conformation, e.g., a helix, in THF at +50 °C. The broad UV−vis absorption band is probably due to the inhomogeneity of the backbone conformations with the various effective conjugation lengths. However, on lowering the solution temperature, the broad UV−vis band changed gradually into well-resolved bands exhibiting red shifts at the wavelength of the absorption peak; the single positive-sign CD band gradually changed into an apparent bisignate CD signal. For example, the CD spectrum at −80 °C exhibits a positive-sign CD signal at a shorter wavelength of 355 nm ($\Delta\epsilon = 2.4$) and

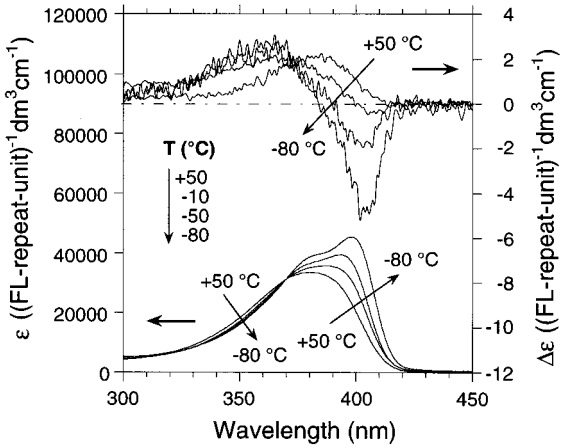

Figure 1. Variable temperature CD and UV−vis spectra of PFMO in THF ($c = 3.0 \times 10^{-5}$ M of the FL repeat unit, path length of 1.0 cm above −10 °C and 0.5 cm below −20 °C, respectively).

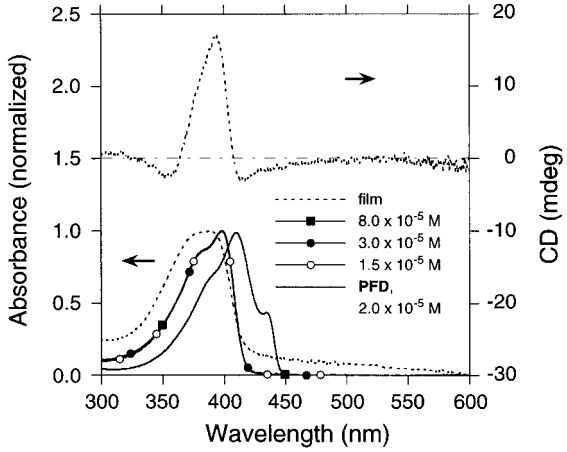

Figure 2. UV−vis and CD spectra of PFMO in a thin film at −80 °C, which is prepared by spin-coating on a quartz substrate from a 1.0×10^{-2} M THF solution, 3000 rpm/min, 30 s; UV−vis spectra of PFMO in THF at three concentrations at −80 °C; UV−vis spectrum of PFD in THF at −60 °C.

a negative one at a longer wavelength of 403 nm ($\Delta\epsilon = -4.7$), corresponding to the resolved UV−vis band peaking at 399 nm with a shoulder around 380 nm.

Two possible assignments should be considered for the origin of the resolved UV−vis bands at lower temperature: one is the first $\pi-\pi^*$ transition and its vibronic (C=C stretching vibration) sideband; another is the consequence of the different $\pi-\pi^*$ transitions due to different backbone conformational motifs. The existence of a clear isosbestic point at 370 nm in the variable temperature UV−vis spectra indicates the latter possibility. At least two different PF motifs with different excitation energies may coexist in the short wavelength region around 360 and 380 nm. It was reported that, among π-conjugated polymers, vibronic sidebands in the UV−vis absorption can be seen clearly in the regioregular polythiophene with an anti-coplanar π-stacking structure in aggregates and/or in films[14,15] and ladder poly(*p*-phenylene) having a geometrically fixed planar π-structure.[16] Therefore, the resolved absorption band of PFMO at low temperature is ascribed to the different motifs incorporated in the PF backbone, and the vibronic sidebands are probably not observable due to the flexibility of the PF backbone, which is caused by the somewhat rotational freedom in the σ-bonds between the adjacent fluorene rings.

The next question is whether the apparent bisignate CD signal at low temperature originates from the individual PF molecules, aggregates, or both. The continuous changes in the UV−vis and CD absorption profiles upon cooling indicate that the bisignate CD signal is likely due to plural PF motifs with different excitation energies and the opposite handedness incorporated in the individual molecules rather than the aggregates, because in the case of aggregation, abrupt changes in the CD and UV−vis spectra are usually observed.[15,17,18]

A comparison between the UV−vis spectra of PFMO in the film and solution states may be useful to test this idea. As shown in Figure 2, the UV−vis spectrum of PFMO in the film state at −80 °C exhibits a moderately intense tail to a longer wavelength above 430 nm, whereas that of PFMO in THF at −80 °C does not show any such absorption tail, indicating that no significant aggregates formed in solution even at −80 °C. This idea is corroborated by the more significant difference between the CD spectra in the solution and thin film states at −80 °C. Indeed, the aggregates in the film state at −80 °C showed a CD spectrum with three extrema at 352 nm ($\Delta\epsilon = -2.6$), 395 nm ($\Delta\epsilon = +17.1$), and 417 nm ($\Delta\epsilon = -3.0$), which is completely different from that of the THF CD spectrum.

The other evidence is the absence of concentration dependence on the CD and UV−vis spectral shapes and the ϵ and $\Delta\epsilon$ values in THF between +50 and −80 °C.[17a] For example, as shown in Figure 2, the UV−vis spectra of PFMO in THF at −80 °C are almost identical at concentrations of 1.5×10^{-5}, 3.0×10^{-5}, and 8.0×10^{-5} M within experimental error.

To further confirm this conclusion, we compared the UV−vis spectrum of PFMO in THF at −80 °C with that of the PF bearing *n*-decyl side chains, poly[2,7-(9,9-di-*n*-decyl)fluorene] (PFD, $M_w = 211\,300$, $M_n = 88\,100$), in THF at −60 °C. In the −60 °C UV−vis spectrum of PFD, a narrow, well-resolved absorption band peaking at 434 nm newly appeared, in addition to the main band at 411 nm with a shoulder around 380 nm. Such a characteristic absorption profile has already been reported for PFO, due to the formation of an intrachain packing structure of fully extended planar zigzag structures (2_1 helix).[6b,7] Therefore, it is reasonable that PFMO dissolved in the good solvent, THF, has difficulty producing aggregates even at low temperature of −80 °C due to the presence of the branched, bulky side chain structure of (*S*)-2-methyloctyl groups.

Photoluminescence Properties. Figure 3A compares two PL spectra of PFMO in THF at −50 °C and at room temperature. The PL spectrum at room temperature exhibits two peaks at 415.5 and 439.0 nm with a shoulder around 470 nm, while that at −50 °C shows two well-resolved bands at 417.5 and 442.5 nm with a shoulder around 475 nm. The difference in the energy between the 417.5 and 442.5 nm bands is 1353 cm^{-1}. The red shifts in the PL spectra upon cooling suggest that the emitting motif gradually changed into that with lower energy due to increasing of the effective conjugation length, which is caused by the better ordering of the PFMO backbone at lower temperature.

Figure 3B shows the PLA plot of PFMO in THF at room temperature. The plot is very weakly dependent on the wavelength and exhibits a small value of ~0.05 between 250 and 360 nm and a slightly larger value of 0.12 at 400 nm, probably due to the fast energy

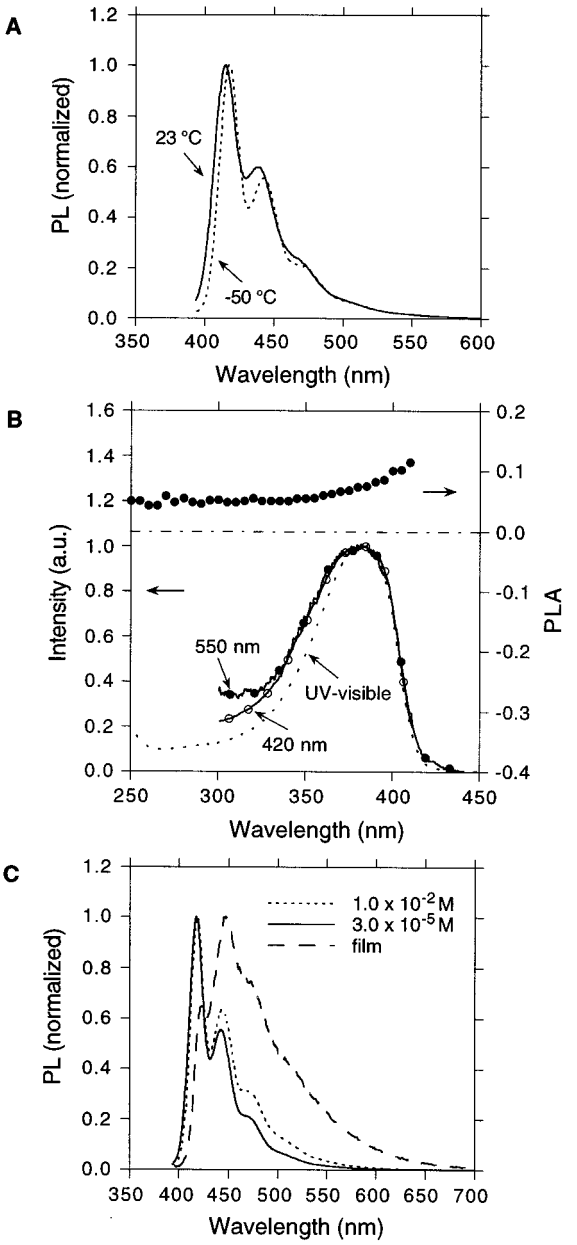

Figure 3. (A) PL spectra of PFMO in THF at room temperature and −50 °C ($c = 3.0 \times 10^{-5}$ M, excitation at 383 nm). (B) PLA plot as a function of wavelength of PFMO in THF, and PLE spectra monitored at 420 and 550 nm emissions together with the UV−vis spectrum of PFMO in THF ($c = 3.0 \times 10^{-5}$ M) at room temperature. (C) PL spectra of PFMO in THF at various concentrations and in a thin film at −50 °C (excitation at 383 nm).

migration within the PF backbone motifs from the shorter conjugated ones with higher energy to the longest conjugated motifs with the lowest energy. This may be related to the observation that the PL spectra are insensitive to the excitation wavelength.

Further PL studies support the above idea that PFMO is dispersed molecularly in THF at a concentration of $\sim 3.0 \times 10^{-5}$ M. One form of evidence is the fact that the PLE spectra are independent of the emission wavelengths.[19] For example, as shown in Figure 3B, the PLE spectrum monitored at 420 nm emission ($c = 3.0 \times 10^{-5}$ M) in THF at room temperature is almost identical to that monitored at 550 nm emission. Another form of evidence is that the PL spectra of PFMO in THF at concentrations between 3.0×10^{-6} and 1.0×10^{-3} M

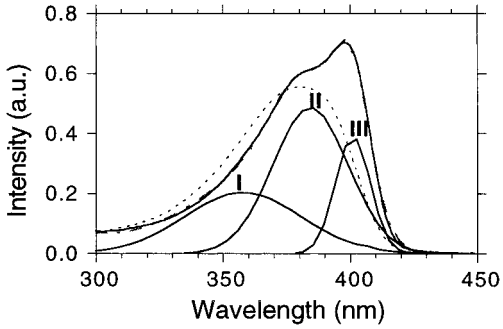

Figure 4. UV−vis spectrum of PFMO in THF at −80 °C and the deconvoluted curves (solid line). UV−vis spectrum of PFMO in THF at +50 °C (normalized for comparison, dotted line).

do not exhibit any featureless emission bands at the longer wavelength around 550 nm. The featureless emission band is generally ascribed to the ground state aggregates and/or the excited state excimers and significantly appears in the PL spectra of PFMO in a thin film and in THF solutions at higher concentrations above 1.0×10^{-3} M.[6] As an example, Figure 3C compares the PL spectra of PFMO in THF solution at low and high concentrations and in a thin film at −50 °C.

Viscometric Study. To qualitatively determine the global conformation of PFMO in solution, the viscometric measurement is useful. The high viscometry index, α, of 1.07 indicates a wormlike structure of PFMO in THF even at +30 °C, as well as such PFs as PFH, PFO, and PFEH. Consequently, it is believed that the PF backbones adopt much stiffer structures at lower temperatures, relating to the apparent bisignate CD signals and the red-shifted UV−vis absorption bands at −80 °C.

Thermodriven Conformational Transition. To elucidate the structures responsible for the positive-sign CD signal at 355 nm and the negative-sign one at 403 nm in the CD spectrum of PFMO in THF at −80 °C, it is necessary to perform peak fitting of the corresponding UV−vis spectrum. Initially, we attempted to perform the peak fitting using the two UV bands centered at 355 and 403 nm but failed to reproduce the original spectrum. Therefore, we tried to perform this operation using three deconvoluted curves centered at 355, 380, and 403 nm and successfully obtained the deconvoluted curves as shown in Figure 4. This is probably because that two PF backbone motifs with different excitation energies may coexist in the short wavelength region around 360 and 380 nm, evidenced by the clear isosbestic point at 370 nm in the variable temperature UV−vis spectra (Figure 1).

The deconvoluted curves indicate that the $\pi-\pi^*$ transitions of PFMO in THF at −80 °C constitute three $\pi-\pi^*$ transitions, corresponding to band I with $\lambda_{max} = 355$ nm, band II with $\lambda_{max} = 380$ nm, and band III with $\lambda_{max} = 403$ nm. On the other hand, the $\pi-\pi^*$ transitions in THF at +50 °C seems to consist mainly of two $\pi-\pi^*$ transitions, corresponding to bands I and II.

Figure 5 shows the changes in the intensities of the CD and UV−vis spectra at three maximum wavelengths as a function of solution temperature. On lowering the temperature from +50 to −80 °C, the ϵ value at the shorter wavelength of 355 nm gradually decreased, but that at the longer wavelength of 380 nm gradually increased, especially that at 403 nm increased signifi-

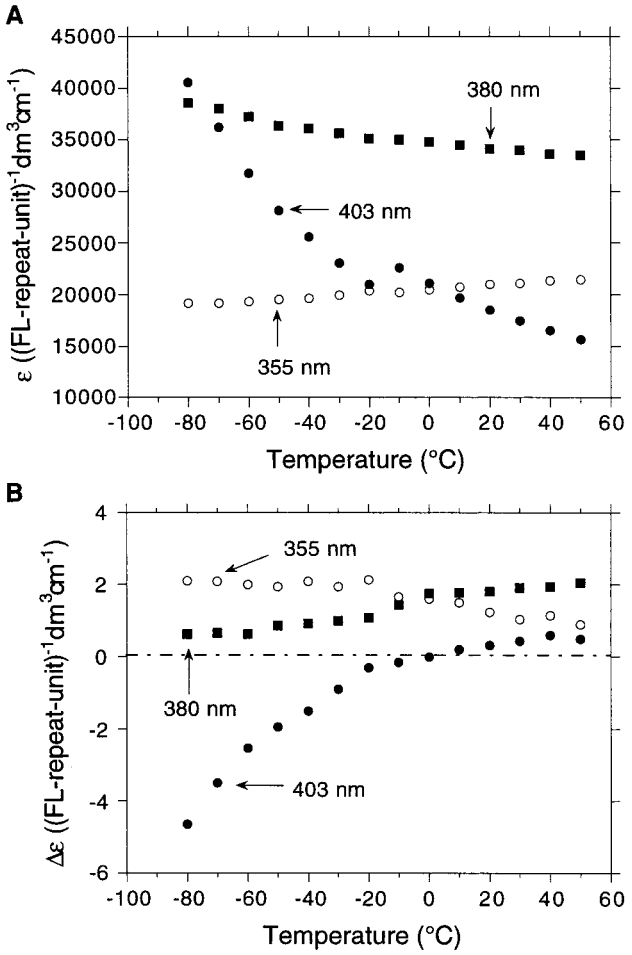

Figure 5. Thermodriven changes in the UV−vis (A) and CD (B) absorptions of PFMO in THF ($c = 3.0 \times 10^{-5}$ M). The discontinuous changes between −10 and −20 °C are probably due to experimental error from the different cells used and the different ratios of the temperature decrease.

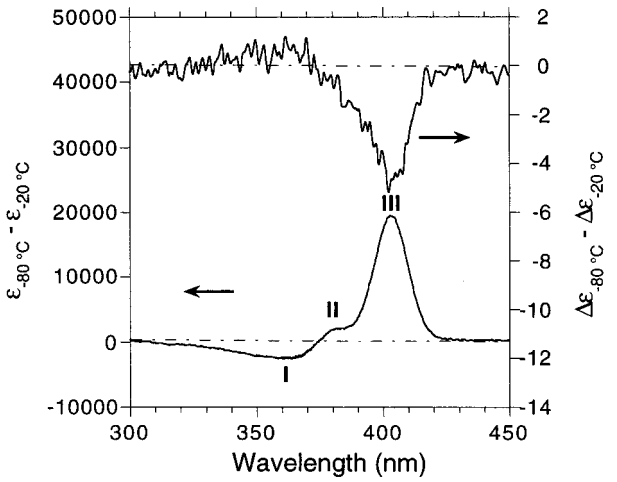

Figure 6. Difference spectra obtained by subtracting the UV−vis and CD spectra at −20 °C from the corresponding spectra at −80 °C.

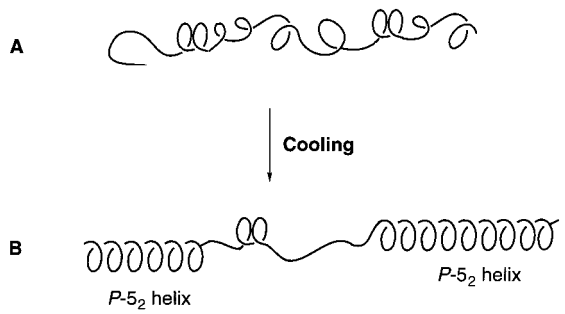

Figure 7. Schematic models of the thermodriven conformational transition from (A) disordered local motifs with overall *M*-helicity in the stiff wormlike PF backbone to (B) a highly ordered PF backbone motif of a P-5_2 helix along with other unclear local PF backbone motifs.

cantly (Figure 5A); the $\Delta\epsilon$ value at 355 nm gradually increased and then remained at an almost constant value starting from −20 °C, that at 380 nm decreased gradually, and that at 403 nm shifted drastically from a positive value of 0.8 to a large negative value of −4.7 through zero at 0 °C (Figure 5B). These UV−vis and chiroptical changes indicate that PFMO in THF solution may undergo a certain thermodriven conformational transition around 0 °C.

Figure 6 shows the difference spectra obtained by subtracting the UV−vis and CD spectra at −20 °C from the corresponding ones at −80 °C. The difference UV−vis spectrum clearly exhibits a sharp positive peak at 403 nm with a full width at half-maximum, fwhm, of 15.6 nm (0.12 eV), which perfectly matches the negative sharp band at 403 nm in the difference CD spectrum. This may be related to the progressive growth of a motif (corresponding to band III at 403 nm) upon cooling from −20 to −80 °C. On the other hand, the weak negative band around 360 nm and the weak positive shoulder around 380 nm in the difference UV−vis spectrum are respectively due to the decrease in ϵ at 355 nm (corresponding to band I at 355 nm) and the increase in ϵ at 380 nm (corresponding to band II at 380 nm), while the difference CD spectrum shows less significant bands at 355 and 380 nm, due to the near invariability in $\Delta\epsilon$ at 355 and 380 nm from −20 to −80 °C. Therefore, we concluded that, upon cooling from −20 to −80 °C, the planarization of the local motifs having λ_{max} values of 355 and 380 nm resulted in the formation of a highly ordered motif. The highly ordered structure at 403 nm is assumed to be a P-5_2 helix (the *P*-handedness is assumed here corresponding to the negative-sign CD band, and vice versa),[8,9] which shows Kuhn's dissymmetry ratio, g_{abs} ($= (\Delta\epsilon_{-80} - \Delta\epsilon_{-20})/(\epsilon_{-80} - \epsilon_{-20})$, defined here), of -2.7×10^{-4}, having a large absolute value.[20] This value is typical for rodlike helical organopolysilanes with single-screw-sense in solution.[20]

Although PFMO may assume a stiff wormlike structure in THF at high temperature of +50 °C, several local motifs would coexist in the PF backbone (Figure 7A), e.g., helically structural precursors (for example, looser *M*- and/or P-5_1 and 5_2), exact alternately twisted (AT) structures (optically inactive),[9,21] and AT structural precursors with different torsional angle (ϕ) values along the local motifs (optically active), due to the somewhat free rotation in the σ-bonds between the adjacent fluorene rings. Consequently, although the exact structures responsible for the bands I and II are difficult to assign, the origins of the two bands may be due to the mixing of such local plural motifs. The bulky (*S*)-2-methyloctyl side chains are expected to lead to excess *M*-handed structures, resulting in the weak positive-sign CD signal at +50 °C.

However, upon cooling the THF solution of PFMO from +50 to −80 °C, the backbone (Figure 7B) is expected to become much stiffer, and the local motifs gradually transformed into a highly ordered structure,

possibly a P-5_2 helix,[8,9] along with other unclear local motifs with the opposite screw sense.[22] The highly ordered motif responsible for the band III at 403 nm formed gradually at the expense of other local motifs, corresponding to the bands I at 355 nm and II at 380 nm.

Conclusions

We reported the first solution state CD spectrum of a newly designed PF featuring highly enantiopure β-branched chiral alkyl side chains, PFMO, in dilute THF solution. Upon cooling the solution temperature from +50 to −80 °C, the broad UV−vis band centered at 380 nm changed into a resolved band peaking at 399 nm with a shoulder around 380 nm; the single positive-sign CD band gradually changed into an apparent bisignate CD signal. PL studies indicated that the energy migration along the PF backbones proceeded rapidly and that the emitting backbone motifs with the lowest energy gradually changed into those having longer conjugation lengths at lower temperature. The high viscosity index of 1.07 for PFMO in THF at +30 °C revealed a stiff, wormlike structure. PFMO in THF solution underwent a certain thermodriven, order−disorder conformational transition with a weak cooperativity around 0 °C. It was considered that, upon cooling, the randomly twisted local motifs in the wormlike PF backbone at higher temperature were transformed into a highly ordered PF backbone motif, possibly a P-5_2 helix, along with other unclear local motifs with the opposite screw sense at lower temperature.

Acknowledgment. We gratefully thank Dr. Kazuaki Furukawa for his kind instructions on low-temperature PL measurements and valuable discussions, Masao Motonaga for his assistance, and Prof. Alex K.-Y. Jen at University of Washington for his generous support and valuable discussions.

References and Notes

(1) (a) Kraft, A.; Grimsdale, A. C.; Holmes, A. B. *Angew. Chem., Int. Ed. Engl.* **1998**, *37*, 402. (b) Friend, R. H.; Gymer, R. W.; Holmes, A. B.; Burroughes, J. H.; Marks, R. N.; Taliani, C.; Bradley, D. D. C.; Dos Santos, D. A.; Brédas, J. L.; Lögdlund, M.; Salaneck, W. R. *Nature (London)* **1999**, *397*, 121. (c) Heeger, A. J. *Solid State Commun.* **1998**, *107*, 673.

(2) Hide, F.; Schwartz, B. J.; Díaz-García, M. A.; Heeger, A. J. *Synth. Met.* **1997**, *91*, 35.

(3) (a) Pei, Q.-B.; Yang, Y.; Yu, G.; Zhang, C.; Heeger, A. J. *J. Am. Chem. Soc.* **1996**, *118*, 3922. (b) Arias, A. C.; MacKenzie, J. D.; Stevenson, R.; Halls, J. J. M.; Inbasekaran, M.; Woo, E. P.; Richards, D.; Friend, R. H. *Macromolecules* **2001**, *34*, 6005.

(4) (a) González-Ronda, L.; Martin, D. C.; Nanos, J. I.; Politis, J. K.; Curtis, M. D. *Macromolecules* **1999**, *32*, 4558. (b) Garnier, F.; Hajlaoui, R.; Yassar, A.; Srivastava, P. *Science* **1994**, *265*, 1684.

(5) (a) McQuade, D. T.; Pullen, A. E.; Swager, T. M. *Chem. Rev.* **2000**, *100*, 2537. (b) Wang, B.; Wasielewski, M. R. *J. Am. Chem. Soc.* **1997**, *119*, 12. (c) Yang, J.-S.; Swager, T. M. *J. Am. Chem. Soc.* **1998**, *120*, 11864.

(6) For recent examples and leading references, see: (a) Fukuda, M.; Sawada, K.; Yoshino, K. *Jpn. J. Appl. Phys.* **1989**, *28*, L1433. (b) Neher, D. *Macromol. Rapid Commun.* **2001**, *22*, 1365. (c) Leclerc, M. *J. Polym. Sci., Part A: Polym. Chem.* **2001**, *39*, 2867. (d) Tang, H.-Z.; Fujiki, M.; Zhang, Z.-B.; Torimitsu, K.; Motonaga, M. *Chem. Commun.* **2001**, 2426. (e) Tang, H.-Z.; Fujiki, M.; Motonaga, M.; Torimitsu, K. *Polym. Prepr.* (*Am. Chem. Soc., Polym. Sci. Div.*) **2001**, *42* (1), 440. (f) Pei, Q.-B.; Yang, Y. *J. Am. Chem. Soc.* **1996**, *118*, 7416. (g) Teetsov, J.; Fox, M. A. *J. Mater. Chem.* **1999**, *9*, 2117. (h) Zhan, X.-W.; Liu, Y.-Q.; Zhu, D.-B.; Jiang, X.-Z.; Jen, A. K.-Y. *Synth. Met.* **2001**, *124*, 323. (i) Teetsov, J. A.; Bout, D. A. V. *J. Am. Chem. Soc.* **2001**, *123*, 3605. (j) Donat-Bouillud, A.; Lévesque, I.; Tao, Y.; D'Iorio, M.; Beaupré, S.; Blondin, P.; Ranger, M.; Bouchard, J.; Leclerc, M. *Chem. Mater.* **2000**, *12*, 1931. (k) Setayesh, S.; Grimsdale, A. C.; Weil, T.; Enkelmann, V.; Müllen, K.; Meghdadi, F.; List, E. J. W.; Leising, G. *J. Am. Chem. Soc.* **2001**, *123*, 946. (l) Xia, C.-J.; Advincula, R. C. *Macromolecules* **2001**, *34*, 5854. (m) Marsitzky, D.; Vestberg, R.; Blainey, P.; Tang, B. T.; Hawker, C. J.; Carter, K. R. *J. Am. Chem. Soc.* **2001**, *123*, 6965. (n) Redecker, M.; Bradley, D. D. C.; Inbasekaran, M.; Woo, E. P. *Appl. Phys. Lett.* **1998**, *73*, 1565.

(7) (a) Grell, M.; Bradley, D. D. C.; Ungar, G.; Hill, J.; Whitehead, K. S. *Macromolecules* **1999**, *32*, 5810. (b) Grell, M.; Bradley, D. D. C.; Long, X.; Chamberlain, T.; Inbasekaran, M.; Woo, E. P.; Soliman, M. *Acta Polym.* **1998**, *49*, 439. (C) Cadby, A. J.; Lane, P. A.; Mellor, H.; Martin, S. J.; Grell, M.; Giebeler, C.; Bradley, D. D. C.; Wohlgenannt, M.; An, C.; Vardeny, Z. V. *Phys. Rev. B* **2000**, *62*, 15604. (d) Cadby, A. J.; Lane, P. A.; Wohlgenannt, M.; An, C.; Vardeny, Z. V.; Bradley, D. D. C. *Synth. Met.* **2000**, *111*, 515. (e) Ariu, M.; Lidzey, D. G.; Bradley, D. D. C. *Synth. Met.* **2000**, *111*, 607. (f) Grell, M.; Bradley, D. D. C.; Inbasekaran, M.; Ungar, G.; Whitehead, K. S.; Woo, E. P. *Synth. Met.* **2000**, *111*, 579.

(8) Lieser, G.; Oda, M.; Miteva, T.; Meisel, A.; Nothofer, H.-G.; Scherf, U.; Neher, D. *Macromolecules* **2000**, *33*, 4490.

(9) Hong, S. Y.; Kim, D. Y.; Kim, C. Y.; Hoffmann, R. *Macromolecules* **2001**, *34*, 6474.

(10) Klaerner, G.; Miller, R. D. *Macromolecules* **1998**, *31*, 2007.

(11) Fytas, G.; Nothofer, H.-G.; Scherf, U.; Vlassopoulos, D.; Meier, G. *Macromolecules* **2002**, *35*, 481.

(12) (a) Oda, M.; Nothofer, H.-G.; Lieser, G.; Scherf, U.; Meskers, S. C. J.; Neher, D. *Adv. Mater.* **2000**, *12*, 362. (b) Oda, M.; Meskers, S. C. J.; Nothofer, H.-G.; Scherf, U.; Neher, D. *Synth. Met.* **2000**, *111*−*112*, 575.

(13) The thermochromic experiments have also been conducted in chloroform and in toluene. Similar positive-sign CD signals in chloroform at +50 °C and/or in toluene at +80 °C, matching their UV−vis absorption peaks, were observed (λ_{max} = 379 nm, $\Delta\epsilon$ = 2.75 in chloroform at +50 °C; λ_{max} = 376 nm, $\Delta\epsilon$ = 3.62 in toluene at +80 °C). On lowering the sample temperature in chloroform and in toluene, similar thermodriven changes in the UV−vis and CD spectra were also seen. However, the chloroform solutions at concentrations ranging from 8.0×10^{-5} to 1.5×10^{-5} M below −20 °C and the toluene solutions at concentrations from 3.0×10^{-4} to 1.5×10^{-5} M below 0 °C led to a rising of the UV−vis spectrum baselines, indicating that scattering phenomena occurred due to aggregates and/or precipitates formed at such a low temperature.

(14) (a) Rughooputh, S. D. D. V.; Hotta, S.; Heeger, A. J.; Wudl, F. *J. Polym. Sci., Polym. Phys. Ed.* **1987**, *25*, 1071. (b) Yamamoto, T.; Komarudin, D.; Arai, M.; Lee, B.-L.; Suganuma, H.; Asakawa, N.; Inoue, Y.; Kubota, K.; Sasaki, S.; Fukuda, T.; Matsuda, H. *J. Am. Chem. Soc.* **1998**, *120*, 2047. (c) Lévesque, I.; Bazinet, P.; Roovers, J. *Macromolecules* **2000**, *33*, 2952. (d) Sakurai, K.; Tachibana, H.; Shiga, N.; Terakura, C.; Matsumoto, M.; Tokura, Y. *Phys. Rev. B* **1997**, *56*, 9552.

(15) Langeveld-Voss, B. M. W.; Janssen, R. A. J.; Meijer, E. W. *J. Mol. Struct.* **2000**, *521*, 285.

(16) Wohlgenannt, M.; An, C. P.; Vardeny, Z. V. *J. Phys. Chem. B* **2000**, *104*, 3846.

(17) (a) Zhang, Z.-B.; Fujiki, M.; Motonaga, M.; Nakashima, H.; Torimitsu, K.; Tang, H.-Z. *Macromolecules* **2002**, *35*, 941. (b) Fiesel, R.; Halkyard, C. E.; Rampey, M. E.; Kloppenburg, L.; Studer-Martinez, S. L.; Scherf, U.; Bunz, U. H. F. *Macromol. Rapid Commun.* **1999**, *20*, 107. (c) Bidan, G.; Guillerez, S.; Sorokin, V. *Adv. Mater.* **1996**, *8*, 157. (d) Langeveld-Voss, B. M. W.; Waterval, R. J. M.; Janssen, R. A. J.; Meijer, E. W. *Macromolecules* **1999**, *32*, 227. (e) Langeveld-Voss, B. M. W.; Peeters, E.; Janssen, R. A. J.; Meijer, E. W. *Synth. Met.* **1997**, *84*, 611. (f) Sakurai, S.; Goto, H.; Yashima, E. *Org. Lett.* **2001**, *3*, 2379.

(18) PFDMO (M_w = 179 000, M_n = 58 700) showed a very weak positive CD signal ($\Delta\epsilon$ = 1.3 at 391 nm) in isooctane at 0 °C. However, the very weak positive-sign CD signal abruptly changed into a bisignate CD band with a resolved structure at −20 °C, showing a large $\Delta\epsilon$ value of 18.1 at 388 nm, by a factor of 14, probably due to the aggregation behavior occurred, because PFDMO can be dissolved in isooctane only at +80 °C with stirring overnight.

(19) (a) Kim, J.; Swager, T. M. *Nature (London)* **2001**, *411*, 1030. (b) Pauck, T.; Hennig, R.; Perner, M.; Lemmer, U.; Siegner,

U.; Mahrt, R. F.; Scherf, U.; Müller, K.; Bässler, H.; Göbel, E. O. *Chem. Phys. Lett.* **1995**, *244*, 171.
(20) The value is comparable to those for helical polysilylenes (e.g., [(*S*)-2-methylbutyl](*n*-hexyl)polysilylene, $g_{abs} = +2.0 \times 10^{-4}$), see: Fujiki, M. *Appl. Phys. Lett.* **1994**, *65*, 3251.
(21) In the AT structure, the fluorene rings rotate about the rotational axis alternately; i.e., a torsional angle (ϕ) between the adjacent rings is given by $\phi_i = (-1)^{i+1}\phi$.[9]
(22) Similar phenomena of a thermodriven conformational transition have also been reported for stiff molecule systems, such as phenylacetylene oligomers. See: (a) Nelson, J. C.; Saven, J. G.; Moore, J. S.; Wolynes, P. G. *Science* **1997**, *277*, 1793. (b) Prince, R. B.; Saven, J. G.; Wolynes, P. G.; Moore, J. S. *J. Am. Chem. Soc.* **1999**, *121*, 3114. The theoretical studies have already been carried out. See: (a) Teramoto, A. *Prog. Polym. Sci.* **2001**, *26*, 667. (b) Yoshikawa, K.; Noguchi, H. *Chem. Phys. Lett.* **1997**, *278*, 184.

MA020327F